International Journal of Pharmaceutics 378 (2009) 116–121

Contents lists available at ScienceDirect

International Journal of Pharmaceutics

journal homepage: www.elsevier.com/locate/ijpharm

Levitated single-droplet drying: Case study with itraconazole dried in binary organic solvent mixtures

Eva Wulsten[b], Filip Kiekens[a], Frederic van Dycke[a], Jody Voorspoels[a], Geoffrey Lee[b,*]

[a] Johnson & Johnson Pharmaceutical R&D, Beerse, Belgium
[b] Division of Pharmaceutics, Friedrich-Alexander-University, Erlangen, Germany

ARTICLE INFO

Article history:
Received 31 August 2008
Received in revised form 26 May 2009
Accepted 26 May 2009
Available online 6 June 2009

Keywords:
Spray drying
Droplet drying
Particle morphology
Levitation

ABSTRACT

The objective of this case study of the single-droplet drying of two itraconazole/polymer formulations was to determine how the solvent system influences drying rate and dried particle morphology. A clear dual functionality of the two solutes could be identified. The polymeric component (PVP or HPMC) determined drying rate, whereas the drug determined end particle morphology. This could be related to solubilities of the two components in the binary solvent mixtures used. The formulation of a surface skin early on in drying only occurred with HPMC and strongly influenced drying rate but not dried particle morphology.

1. Introduction

Single-droplet drying is the only technique that is suitable for the quantitative examination of both the drying rate and particle genesis from a solution intended for spray drying. The use of acoustic levitation allows free suspension of the single droplet in a drying gas (Kastner et al., 2001), and avoids thereby the artifacts in heat transfer that occur with capillary suspension techniques (Ranz and Marshall, 1952). The single droplet is levitated in the nodal region of a standing acoustic wave where it can be held stable during conductional or convective drying in the surrounding gas. This technique has been successfully used to examine the drying behaviour of solvent droplets (Tuckermann et al., 2002; Schiffter and Lee, 2007a), aqueous suspensions (Kastner et al., 2001), and – in the field of pharmacy – aqueous solutions of carbohydrates or proteins (Schiffter and Lee, 2007b).

The single droplet acoustic levitator has a potential application in the field of process development of spray drying. It is possible to examine solution droplet drying behaviour under drying conditions close to those existing within a spray-drying chamber (Schiffter and Lee, 2007a). A study with carbohydrates and proteins showed, for example, a striking similarity between particle morphologies obtained from the acoustic levitator and a mini-scale spray-dryer (Schiffter and Lee, 2007b) In this paper we present a case study that gives an example of how measurements of single solution-droplet drying with the acoustic levitator can provide relevant information about the effects of formulation on particle morphology that is relevant to process development. Itraconazole is to be formulated with either polyvinylpyrrolidon or hydroxypropyl methylcellulose as a spray-dried powder suitable for storage and further processing. Some preliminary studies had identified a binary solvent mixture of dichloromethane plus ethanol in which the polymeric formulations could be spray-dried on a pilot-scale machine. The spray-dried powders showed, however, substantial differences in their appearance depending on both the polymer and the composition of the binary solvent mixture. The objective of this study with the single-droplet drying levitator was to determine if these two factors produce different solution-droplet drying behaviour that could be related to different dried particle morphology. Although polymers are frequently used as ingredients of spray-dried formulations (Tewa-Tagne et al., 2007) there is no published work on single-droplet drying to visualize particle genesis from polymer solutions. The results obtained in this work reveal substantial differences between the drying behaviour of the two polymers examined, and also the strong effect of solvent composition.

2. Materials and methods

2.1. Materials

Itraconazole was obtained from Janssen Pharmaceutical (Belgium) and used as received. Polyvinylpyrrolidon ($PVP_{co}VA$) (Kollidon VA64; batch 59933416KO) of molecular weight 45–70 kDa was

* Corresponding author. Tel.: +49 9131 85 295 52; fax: +49 9131 85 295 45.
E-mail address: lee@pharmtech.uni-erlangen.de (G. Lee).
URL: http://www.pharmtech.uni-erlangen.de (G. Lee).

0378-5173/$ – see front matter © 2009 Elsevier B.V. All rights reserved.
doi:10.1016/j.ijpharm.2009.05.060

Table 1
Compositions of the solution droplets examined in this work. In all cases the solvent used for these solutions was the binary mixtures of dichloromethane/ethanol.

Formulation #	Itraconazole [% w/w]	$PVP_{co}VA$ [% w/w]	HPMC [% w/w]
1	3.182	4.773	0
2	3.182	0	4.773
3	0	4.773	0
4	0	0	4.773

obtained from BASF (Ludwigshafen, Germany), and hydroxypropyl methylcellulose 2910 5 mPa s (Pharmacoat 615; batch 20022509) of molecular weight 15 kDa from Dow Chemicals (Midland, USA). Dichloromethane and ethanol (99%) were obtained from Roth Chemicals (Berlin, Germany) and were of analysis grade.

2.2. Levitated single-droplet drying

The single-droplet drying ultrasonic levitator is based on a literature design (Kastner et al., 2001) and has been fully described in a previous publication (Schiffter and Lee, 2007a). Briefly, a solvent or solution droplet of approximately 1000 μm diameter is levitated in the region of the second node of the standing acoustic wave produced between a 57 Hz transducer and a reflector contained in an acrylic glass chamber. In this study the levitator chamber was filled with dry nitrogen gas whose temperature (T_d) and flow rate (u_d) were adjusted using a controlled evaporation mixer (CEM). Images of the drying droplet were taken at 5 Hz using a CCD video camera. The surface temperature of the drying droplet was measured using infra-red thermography, as described before (Wulsten and Lee, 2008). The interested reader is referred to references (Schiffter and Lee, 2007a; Schiffter and Lee, 2007b) and (Wulsten and Lee, 2008) for full details of this technique.

The levitator chamber was first warmed up to its operating conditions of T_d = 50 °C and u_d = 0 L/min. A single droplet was produced on the tip of a Hamilton syringe and introduced into the levitator chamber and levitated at the second node of the standing acoustic wave. During the course of droplet drying the following parameters were determined: the droplet's horizontal and vertical diameters, D_h and D_v, respectively, and the droplet surface temperature across the droplet profile, T_s. At the end of each experiment with a solution droplet the dried particle was recovered from the levitator chamber and examined by scanning electron microscopy on an Amray 1810T at 20 kV after 5 min Au sputtering at 20 mA/5 kV (Hummer JR Techniques).

In the first series of experiments the drying kinetics of the binary solvent mixture of dichloromethane and ethanol in various weight fractions were determined. The second series examined the drying kinetics and particle genesis of an itraconazole/$PVP_{co}VA$ formulation in the binary solvent mixtures, and the third series of an itraconazole/HPMC formulation. The details of the compositions of the two formulations are given in Table 1.

3. Results and discussion

3.1. Drying kinetics of binary solvent mixtures

A droplet levitated in a standing acoustic wave is deformed to the shape of an oblate spheroid by the asymmetric horizontal and vertical levitation forces acting on it (Tian et al., 1993). The measured values of D_h and D_v were therefore used to calculate the surface-equivalent spherical droplet radius, $r(t)$. For a spherical solvent droplet of initial radius r_0 evaporating in still gas of constant temperature, T_d, the evaporation rate is given by the steady-state d^2-law (Frohn and Roth, 2000):

$$\frac{r^2(t)}{r_0^2} = 1 - \left\{ \frac{2DM}{\rho R} \left(\frac{P_s}{T_s} - \frac{P_d}{T_d} \right) \right\} \frac{t}{r_0^2} \quad (1)$$

M is the solvent's molecular weight and ρ its density, D is the diffusivity [cm^2/s] of the solvent vapour in the drying gas, R is the gas constant, T_s is the droplet surface temperature, P_s is the partial vapour pressure of the solvent at the droplet surface, and P_d is its partial vapour pressure in the drying gas phase. Fig. 1a shows the corresponding plots of $r^2(t)/r_0^2$ versus t/r_0^2 for the various binary mixtures of dichloromethane (DCM) and ethanol (EtOH) in the range DCM/EtOH (90:10) to (0:100) by weight. The pure DCM (i.e. 100:0) could not be determined because the droplet vaporized immediately on introduction into the levitation chamber. DCM's boiling point of 42 °C lies below the T_d of 50 °C used in this experiment. The highest fractions of DCM, viz. (90:10) and (75:25), show biphasic plots in Fig. 1a, weight whereas at the lower weight fractions of DCM the profiles are less curved. This is the behaviour predicted for the drying of droplets of a binary solvent mixture (Yarin et al., 2002) where at early times the more volatile component (in this case the DCM) evaporates preferentially. At later times the profile approaches that of the pure, less-volatile component, i.e. EtOH, as is evident from the plots in Fig. 1a. The result for pure EtOH is also a slight curve, as evident especially at $r^2(t)/r_0^2 \rightarrow 0.5$. This departure from Eq. (1) is caused by an increase in T_s and hence a reduction in $(T_d - T_s)$ during droplet drying (Schiffter and Lee, 2007a), as will be seen presently in Fig. 1c.

The change in drying behaviour with variation in binary solvent composition is clearly illustrated in Fig. 1b by the evaporation coefficient, β [mm^2/s], calculated from the tangents to each plot of $r^2(t)/r_0^2$ at both the start and end points of drying. Both the start and end values for β decrease with higher fraction of EtOH, and converge at (0:100) to that value for pure EtOH. The dependence of the start β on the composition is much greater than that of the end β. This is because the DCM evaporates preferentially at early times and has been largely lost in the end phase of drying. The β of the pure EtOH under the conditions used in the levitator chamber can be directly calculated from:

$$\beta = \frac{2DM}{\rho R} \left(\frac{P_s}{T_s} - \frac{P_d}{T_d} \right) \quad (2)$$

The value for D of EtOH vapour in N_2 gas was calculated according to the method given by Fuller et al. (1966). The value of P_s was calculated from Antoine's equation (Poling et al., 2001) at the measured T_s. At T_d = 50 °C and P_d = 0 the resulting predicted value for β is 0.34×10^{-4} mm^2/s. This lies very close to the measured value in Fig. 1b of 0.33×10^{-4} mm^2/s. Note that in this calculation the measured value of T_s must be used and not the wet-bulb, since use of the latter is inaccurate because of droplet warming in the standing acoustic wave (Wulsten and Lee, 2008). By using the measured T_s the d^2-law gives therefore good agreement with the experimental result of evaporation rate from the acoustic levitator for pure EtOH. Note that the β values for the binary mixtures of DCM/EtOH could not be calculated from Eq. (2) because there are no accurate estimates of P_s available for these mixtures.

The droplet surface temperature must change during drying as the composition of the binary mixture moves towards that of the less-volatile component (Tuckermann et al., 2005). Fig. 1c shows the plots of measured T_s versus t/r_0^2 for the various DCM/EtOH binary solvent mixtures. At (10:90) T_s starts well below zero, before increasing to a brief plateau value of approximately +17 °C after $t/r_0^2 = 60$ s/mm^2. This time point corresponds to that of the change in slope of the $r^2(t)/r_0^2$ plot in Fig. 1a. We observe therefore a good agreement between the changes in T_s and droplet drying rate. If the DCM has been largely lost from this binary mixture after $t/r_0^2 = 60$ s/mm^2, then the drying rate will have decreased since

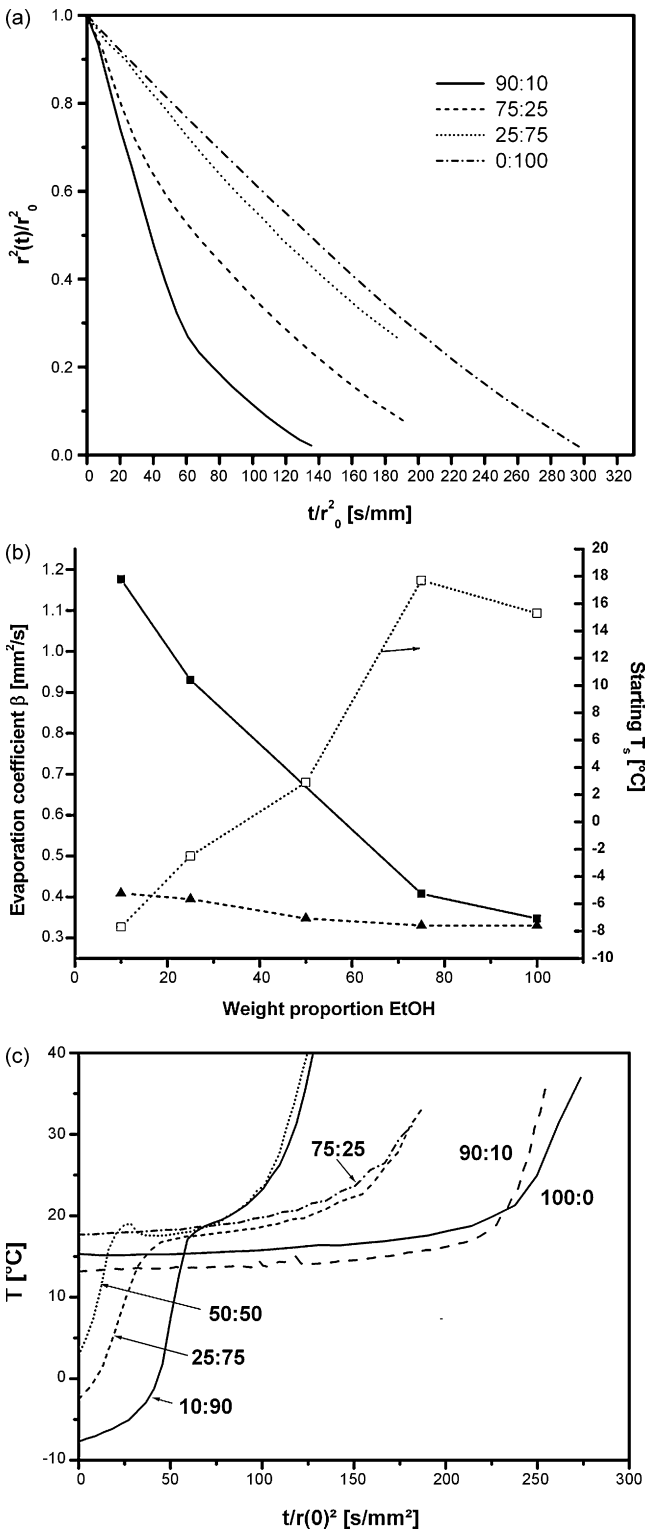

Fig. 1. Levitated single-droplet drying behaviour of binary solvent mixtures of dichloromethane (DCM) and ethanol (EtOH) determined at T_d = 50 °C, 1% RH, and u_{da} = 0 m/s. Symbols: $r(t)$ = droplet radius at time t; r_0 = initial droplet radius at t = 0; T_s = droplet surface temperature; β = evaporation coefficient of initial or terminal slopes of $r^2(t)/r_0^2$ versus t/r_0^2. (a) Drying rate plots of $r^2(t)/r_0^2$ versus t/r_0^2 at various solvent weight proportions (DCM:EtOH). (b) Dependence of β and initial T_s on solvent composition. (c) Profiles of T_s versus t/r_0^2.

the start of drying and T_s will have increased, as observed. At larger fractions of EtOH through (25:75) to (50:50) in Fig. 1c the same T_s profile shape is maintained. The initial T_s's are, however, shifted to higher temperatures. These correspond to the higher boiling points of the binary mixtures containing larger fractions of EtOH. Additionally, the T_s profiles reach the plateau at 17 °C after earlier times since less DCM is available in the starting binary mixtures. At ≥(75:25) the biphasic behaviour in Fig. 1c has been lost and T_s increases steadily until the end of droplet drying. Fig. 1b shows that the start T_s (t = 0) increases linearly with higher fraction of EtOH, indicating near ideal mixing of the two solvents (Tuckermann et al., 2005) and no azeotrope. These results are the first demonstration of how droplet drying rate (β) and surface temperature (T_s) are connected during the drying of microdroplets of such a binary solvent mixture.

3.2. *PVP$_{co}$VA/itraconazole formulation*

The plots of $r^2(t)/r_0^2$ in Fig. 2a obtained from the solution droplets of itraconazole plus PVP$_{co}$VA (formulation # (1) in Table 1) show distinctive 'constant-rate' and 'falling-rate' periods of drying that are separated by a clear critical point (Masters, 1991). With higher fraction of EtOH in the binary solvent mixture (curves 1 → 6) the drying rate tends to decrease and the temporal position of the critical point is shifted to later times. Although this shift is substantial, it can be accounted for by the lower drying rate. Thus, moving from preponderantly DCM, i.e. (90:10), to pure EtOH, i.e. (0:100), approximately doubles the duration of drying to the critical point (cf. Fig. 2a). The β determined during the 'constant-rate' period is approximately halved (cf. Fig. 2b), which agrees with the prediction of boundary layer theory for the quantitative relation between the drying rate and duration of the 'constant-rate' period (Schiffter and Lee, 2007a).

The dependence of the duration of drying to the critical point on the solubility of itraconazole in the solvent is evidently of no great importance. Itraconazole is much more soluble in DCM (250 g/L) than in EtOH (0.2 g/L). Yet moving from (90:10) to (0:100) increases the duration of the constant-rate period. Moving to a solvent that has a higher solubility for a solute should delay the onset of solute precipitation at the droplet surface. This suggests that it is not the itraconazole that determines the temporal position of the critical point in this formulation. The PVP$_{co}$VA is, however, highly soluble in both solvents. Evidently it is the PVP$_{co}$VA and not the itraconazole that determines the precipitation of solid at the droplet surface during drying. This is surprising considering that the both the drug and the polymer are present in almost equal weight concentrations in the solution before drying (cf. Table 1). We suggest that the PVP$_{co}$VA acts as a solvent for the itraconazole, preventing its precipitation as the DCM is preferentially lost during drying. More evidence to support this dominance of the polymer in determining drying behaviour of the solution will be found in the following experiments.

The T_s profiles in Fig. 2a differ greatly from those for the equivalent binary solvent mixtures seen in Fig. 1c. The start solution droplet surface temperatures lie in the range of 16–20 °C, increasing up to the critical point. The start T_s is slightly higher with greater fraction of EtOH in the formulation (see Fig. 2b). Recall from Fig. 1c that the DCM-rich binary solvent droplets have much lower start T_s than that seen in Fig. 2a for the solutions, being sub-zero for (10:90) and (25:75). Indeed, the start T_s lies above 10 °C only in the EtOH-rich binary solvent droplets ≥(75:25). The low start T_s in the DCM-rich binary solvent droplets is a result of preferential evaporation of the more-volatile DCM. This influence of DCM on T_s is greatly reduced in the solution droplets (Fig. 2b) compared with that in the binary solvent droplets (Fig. 1c). This finding is also unexpected and indicates that preferential evaporation of DCM from the DCM-rich solution droplets is hindered by the presence of the solutes.

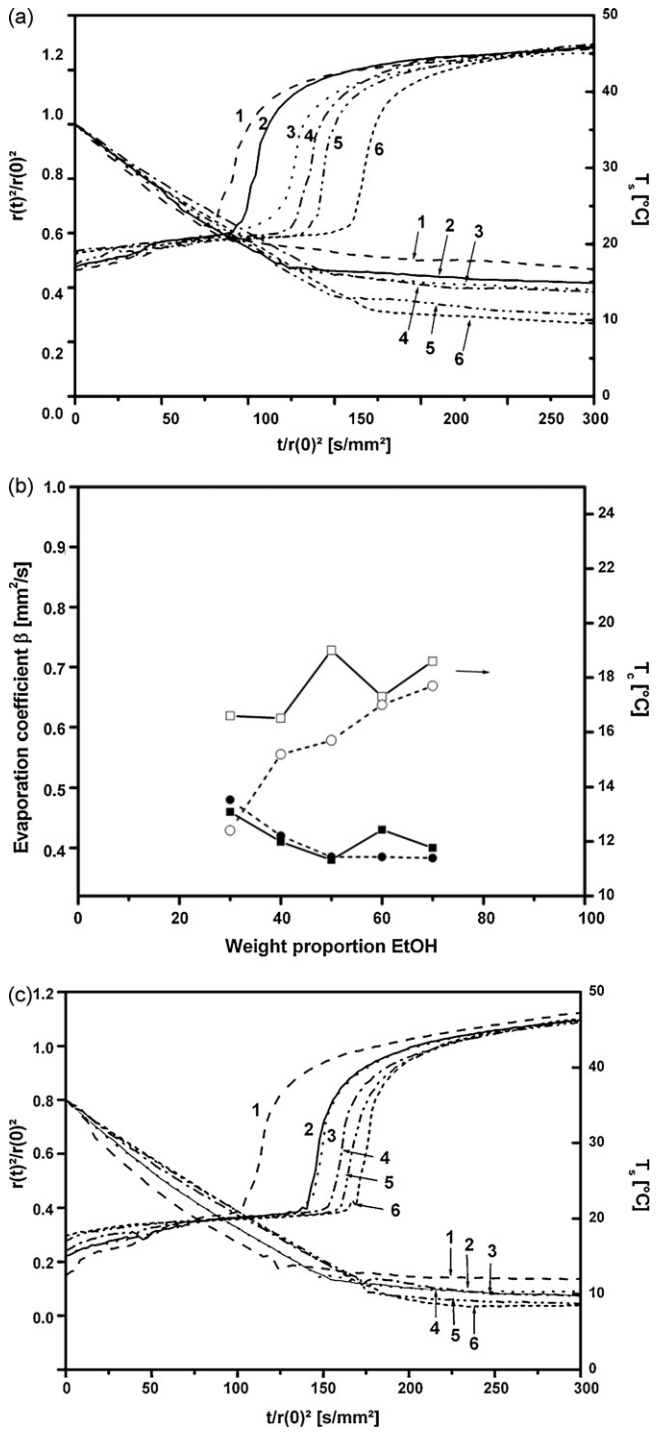

Fig. 2. Droplet drying behaviour of PVP-based formulation in different binary solvent mixtures. Symbols: $r(t)$ = droplet radius at time, t; r_0 = initial droplet radius; T_s = droplet surface temperature; β = evaporation coefficient. (a) Solution of 4.7% (w/w) itraconazole + 3.1% (w/w) PVP dried at T_d = 50 °C. (b) Dependence of β and initial T_s on solvent composition. (c) Solution of 4.7% (w/w) PVP dried at T_d = 50 °C.

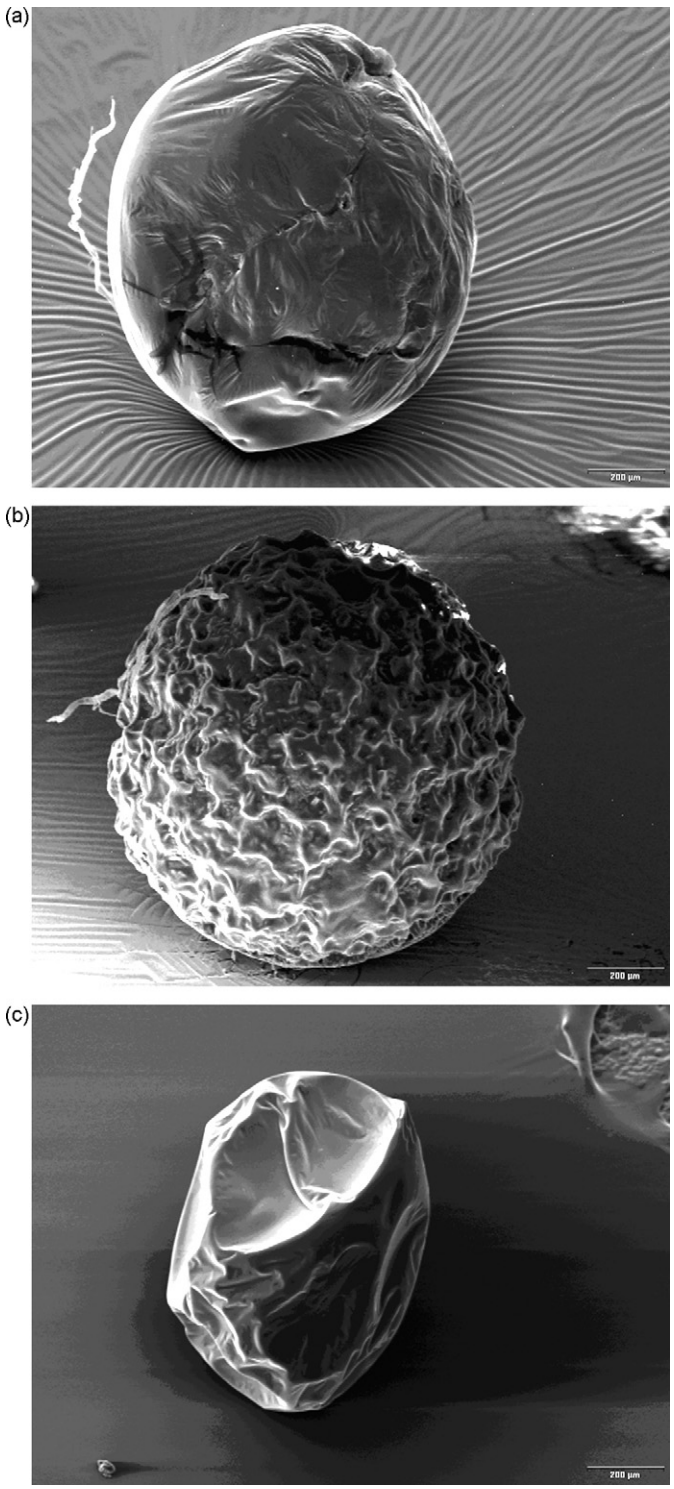

Fig. 3. Scanning electron micrographs of dried particles removed from the levitator chamber at the end of single-droplet drying at T_d = 50 °C. (a) 3.7% (w/w) itraconazole + 4.7% (w/w) PVP in DCM/EtOH (90:10). (b) 3.1% (w/w) itraconazole + 4.7% (w/w) PVP in DCM/EtOH (30:70). (c) 4.7% (w/w) PVP in DCM/EtOH (30:70).

The binary solvent composition influences the morphology of the dried particles of this formulation isolated from the levitator chamber. High fractions of DCM produce a smooth particle surface, as seen in Fig. 3a for the example of (90:10). By increasing the fraction of EtOH the particle surface becomes progressively more structured, for example (30:70) in Fig. 3b. The surface appearance is now that of a network of scaffolding coated with a shrunken pellicle.

Evidence to support the dominating role of the $PVP_{co}VA$ is found by removing itraconazole from the solution (formulation #3 in Table 1). The resulting droplet drying rate (Fig. 2c) is unchanged over that seen with the polymer plus drug (Fig. 2a). Yet the critical point is now shifted to later times, as evident in both the $r^2(t)/r_0^2$ and T_s profiles. This is, however, just the expected result of a lower solids' content of the solution—4.7% (w/w) compared with 7.8% (w/w) for

the itraconazole + PVP$_{co}$VA (cf. Table 1) that prolongs the 'constant-rate' period. It is the evaporation coefficients that are not different from those seen with the PVP$_{co}$VA + itraconazole (Fig. 2b). The profiles of T_s also are unchanged (Fig. 2c), and the plots of start T_s versus fraction of EtOH (Fig. 2b) are hardly altered by removal of the itraconazole. These results confirm that it is the polymer, and not the itraconazole, that determines the drying rate of the solution droplets, despite the almost equal weight concentrations of polymer and drug in solution.

Furthermore, the relatively sharp critical points in the $r^2(t)/r_0^2$ and T_s profiles in Fig. 2c show that the PVP$_{co}$VA precipitates after this time at the droplet surface and immediately reduces the drying rate (Masters, 1991). This is the typical behaviour observed for the single-droplet drying of low molecular weight, amorphous carbohydrates (Schiffter and Lee, 2007b). Up to the critical point the droplet surface remains liquid, yet the dissolved PVP$_{co}$VA greatly reduces evaporation rate compared with the binary solvent mixture. The evaporation coefficients obtained with the PVP$_{co}$VA solutions lie in the range 0.38–0.42 mm^2/s during the 'constant-rate' period (Fig. 2b). These are much lower than the values of start β obtained from the binary solvent mixtures in Fig. 1b. This phenomenon is particularly evident at high fractions of DCM, e.g. ≥(60:40), where β of the PVP$_{co}$VA solutions is low (Fig. 2b) and T_s is high (Fig. 2b). This result agrees with the T_s measurements in Fig. 2a and is a further strong indication that the PVP$_{co}$VA hinders preferential evaporation of DCM in the DCM-rich mixtures. This polymer evidently binds the DCM in solution during drying.

Removal of itraconazole from the formulation does, however, affect the dried particle appearance. The same particle morphology is now observed for all binary solvent compositions, the representative example of (70:30) being given in Fig. 3c. The particle is collapsed and has a smooth surface that no longer shows the structured appearance seen with the drug formulation in Fig. 3b. It is therefore precipitated itraconazole that produces the crystalline-like surface appearance of the itraconazole/PVP$_{co}$VA formulations at high fractions of EtOH, e.g. in Fig. 3b. This has, however, no affect on the drying rate. The PVP$_{co}$VA determines the single-droplet drying rate, whereas the itraconazole only influences the dried particle morphology. These results are the first demonstration of such a dual functionality in single-droplet drying and illustrate the utility of the technique used.

3.3. HPMC/itraconazole formulation

Substitution of PVP$_{co}$VA with HPMC (formulation #2 in Table 1) produces a different single-droplet drying behaviour. The plots of $r^2(t)/r_0^2$ in Fig. 4a show no critical point up to t/r_0^2 of 300 s/mm^2. This is a result of rapid formation of a surface skin that was clearly observed early on in the drying process ($t/r_0^2 < 50$ s/mm^2) with this polymer. This phenomenon must be related to a lower solubility of the polymeric component in the surface layer of the solvent as drying proceeds. With HPMC this leads to rapid precipitation, whereas the PVP$_{co}$VA has sufficient solubility to maintain a liquid surface until much later in drying.

The surface skin strongly the influences drying rate, but not the dried particle appearance. Thus, the evaporation coefficients in Fig. 4b are lower than those determined with the PVP$_{co}$VA formulation (cf. Fig. 2b). This difference in evaporation rate depends on the composition of the binary solvent mixture. It is largest at high fractions of DCM and becomes smaller as pure EtOH is approached. As a result β in Fig. 4b tends to increase with higher fraction of EtOH.

The T_s profiles in Fig. 4a also show no evident critical point. As seen with the PVP$_{co}$VA/itraconazole, the start T_s with the DCM-rich formulations is much higher than the measured values for the pure binary solvent mixtures. This polymer also evidently hinders the preferential evaporation of DCM at early drying times. Since this phenomenon is seen with both polymers, it cannot be caused by the surface skin that is formed only with the HPMC. It is more likely that the polymer binds the DCM in solution during drying.

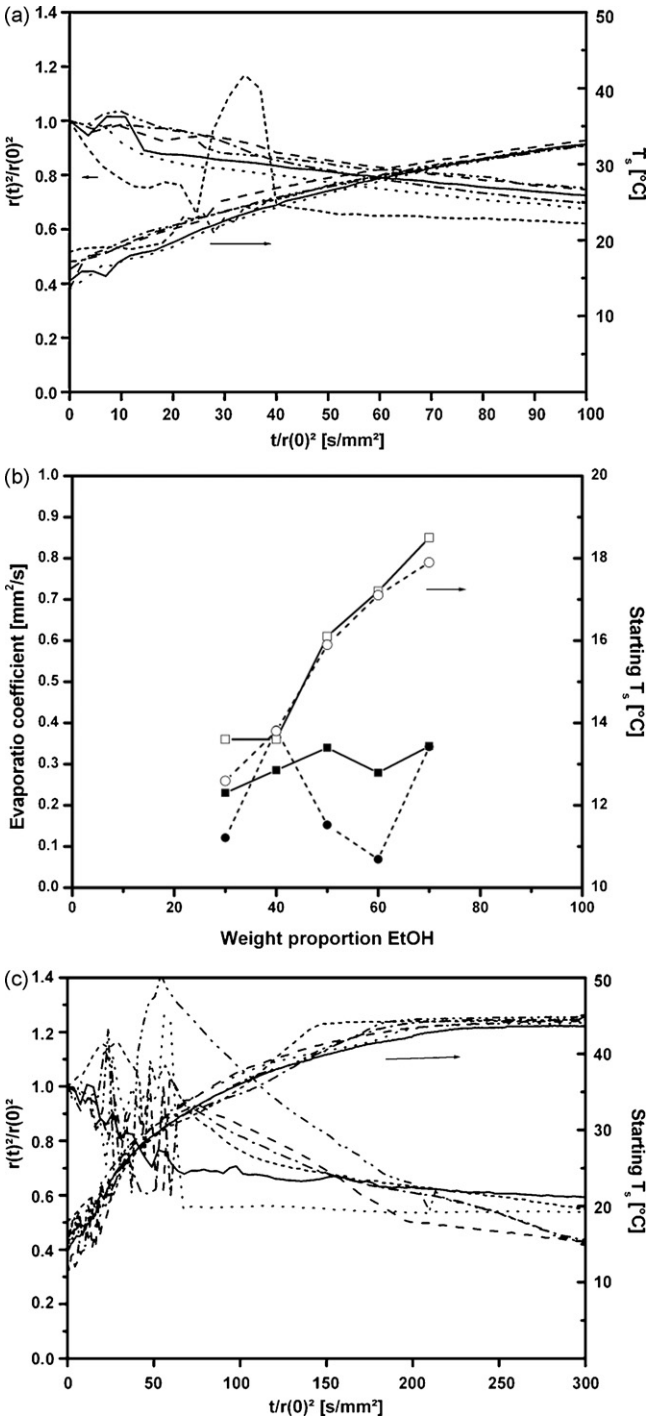

Fig. 4. Droplet drying behaviour of HPMC-based formulation in different binary solvent mixtures. Symbols: $r(t)$ = droplet radius at time, t; r_0 = initial droplet radius; T_s = droplet surface temperature; β = evaporation coefficient. (a) Solution of 4.7% (w/w) itraconazole + 3.1% (w/w) HPMC dried at T_d = 50 °C. (b) Dependence of β and initial T_s on solvent composition. (c) Solution of 4.7% (w/w) HPMC dried at T_d = 50 °C.

The SEM in Fig. 5a of the particle obtained from the (70:30) binary solvent mixture shows that the surface skin has collapsed during the course of drying. A smooth particle surface is observed

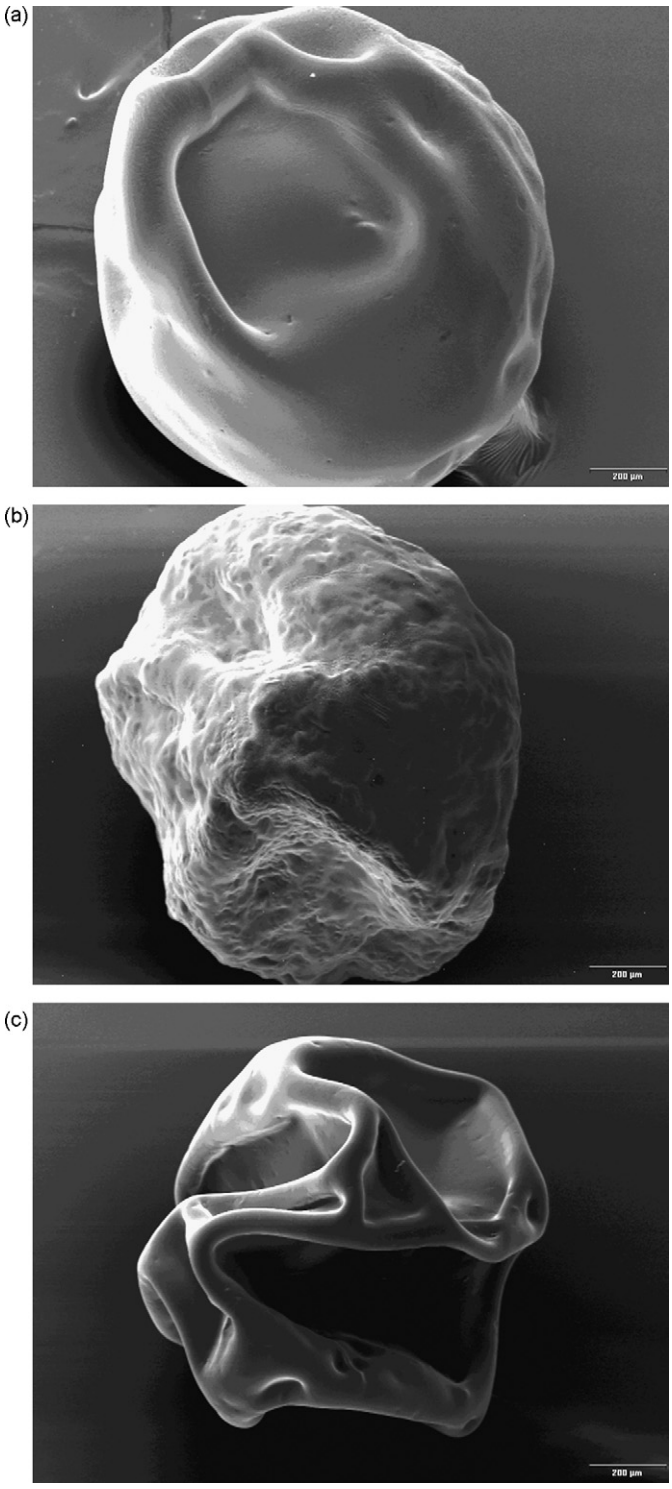

Fig. 5. Scanning electron micrographs of dried particles removed from the levitator chamber at the end of single-droplet drying at $T_d = 50\,^{\circ}C$. (a) 3.7% (w/w) itraconazole + 4.7% (w/w) HPMC in DCM/EtOH (70:30). (b) 3.1% (w/w) itraconazole + 4.7% (w/w) HPMC in DCM/EtOH (40:60). (c) 4.7% (w/w) HPMC in DCM/EtOH (70:30).

with high fractions of DCM ≥(50:50). The appearance of crystalline-like structure is only evident at low fractions of DCM ≤(40:60), for example in Fig. 5b, where the solubility of the itraconazole in the EtOH-rich binary solvent mixtures is low. This behaviour is the same as that seen with the $PVP_{co}VA$/itraconazole, since it is determined by the drug and not the polymer.

The importance of the polymer for drying behaviour can again be realized by removing the itraconazole from the HPMC formulation (formulation #4 in Table 1). This hardly alters drying behaviour: Fig. 4c shows the same profiles of $r^2(t)/r_0^2$ and T_s. The droplet drying progresses slowly and with no critical point of drying. The evaporation coefficients in Fig. 4b are much scattered because of the irregular $r^2(t)/r_0^2$ plots, but do not differ in essence from those of the itraconazole/HPMC solutions. T_s is also high and increases with larger fraction of EtOH (Fig. 4b).

Skin formation was also observed early on during droplet drying, confirming that this phenomenon comes from the HPMC. The dried particles show a collapsed appearance with a smooth surface structure (Fig. 5c for the example of (30:70)) and no crystalline-like appearance at high proportions of EtOH. The itraconazole is therefore responsible for this morphology. The HPMC formulation thus also demonstrates a dual functionality of the two solutes during single-droplet drying.

4. Conclusions

This study demonstrates how the acoustic levitator can be used to resolve effectively the differences in the drying behaviour of two polymeric itraconazole formulations. Of particular interest is the finding that the polymeric component determines the drying rate, whereas the drug has a strong influence on dried particle morphology. The advantage of measurements of single-droplet drying over spray drying experiments is that both the temporal drying rate and a picture of particle formation can be obtained. In the present study it was, for example, possible with HPMC to observe surface skin formation early on in the drying process.

References

Frohn, A., Roth, N., 2000. Dynamics of Droplets. Springer, Berlin, pp. 29–33.
Fuller, E., Schettler, P., Giddings, J., 1966. A new method for prediction of binary gas-phase diffusion coefficients. Ind. Eng. Chem. 58, 19–27.
Kastner, O., Brenn, G., Rensink, D., Tropea, C., 2001. The acoustic tube levitator—a novel device for determining the drying kinetics of single droplets. Chem. Eng. Technol. 24, 335–339.
Masters, K., 1991. Spray Drying Handbook, 5th ed. Longman Scientific & Technical, London, pp. 309–339.
Poling, B., Prausnitz, J., O'Connell, J., 2001. The Properties of Gases and Liquids, 5th ed. McGraw-Hill, NY, p. 7.4.
Ranz, W., Marshall, W., 1952. Evaporation from drops. Chem. Eng. Prog. 48, 141–146.
Schiffter, H., Lee, G., 2007a. Single-droplet evaporation kinetics and particle formation in an acoustic levitator. Part 1. Evaporation of water microdroplets assessed using boundary-layer and acoustic levitation theories. J. Pharm. Sci. 96, 2274–2283.
Schiffter, H., Lee, G., 2007b. Single-droplet evaporation kinetics and particle formation in an acoustic levitator. Part 2. Drying kinetics and particle formation from microdroplets of aqueous mannitol, trehalose, or catalase. J. Pharm. Sci. 96, 2284–2295.
Tewa-Tagne, P., Briancon, S., Fessi, H., 2007. Preparation of redispersible dry nanocapsules by means of spray drying: development and characterisation. Eur. J. Pharm. Sci. 30, 124–135.
Tian, Y., Holt, G., Apfel, R., 1993. Deformation and location of an acoustically levitated liquid drop. J. Acoust. Soc. Am. 93, 3096–3104.
Tuckermann, R., Bauerecker, S., Neidhart, B., 2002. Evaporation rate of alkanes and alkanols from acoustically-levitated drops. Anal. Bioanal. Chem. 372, 122–127.
Tuckermann, R., Bauerecker, S., Cammenga, H., 2005. IR-thermography of evaporating acoustically levitated drops. Int. J. Thermophys. 26, 1583–1594.
Wulsten, E., Lee, G., 2008. Surface temperature of acoustically levitated water microdroplets measured using infra-red thermography. Chem. Eng. Sci. 63, 5420–5424.
Yarin, A., Brenn, G., Rensink, D., 2002. Evaporation of acoustically-levitated droplets of binary liquid mixtures. Int. J. Heat Fluid Flow 23, 471–486.